ELSEVIER

CrossMark

Ultrasound in Med. & Biol., Vol. 41, No. 8, pp. 2259–2265, 2015

0301-5629/$ - see front matter

http://dx.doi.org/10.1016/j.ultrasmedbio.2015.03.025

● *Technical Note*

DELIVERING AGENTS LOCALLY INTO ARTICULAR CARTILAGE BY INTENSE MHZ ULTRASOUND

Heikki J. Nieminen,* Tuomo Ylitalo,*† Jussi-Petteri Suuronen,* Krista Rahunen,† Ari Salmi,* Simo Saarakkala,†‡ Ritva Serimaa,* and Edward Hæggström*

*Department of Physics, University of Helsinki, Helsinki, Finland; †Research Center for Medical Imaging, Physics and Technology, Faculty of Medicine, University of Oulu, Oulu, Finland; and ‡Department of Diagnostic Radiology, Oulu University Hospital, Oulu, Finland

(*Received* 22 *July* 2014; *revised* 18 *March* 2015; *in final form* 27 *March* 2015)

Abstract—There is no cure for osteoarthritis. Current drug delivery relies on systemic delivery or injections into the joint. Because articular cartilage (AC) degeneration can be local and drug exposure outside the lesion can cause adverse effects, localized drug delivery could permit new drug treatment strategies. We investigated whether intense megahertz ultrasound (frequency: 1.138 MHz, peak positive pressure: 2.7 MPa, I_{spta}: 5 W/cm^2, beam width: 5.7 mm at −6 dB, duty cycle: 5%, pulse repetition frequency: 285 Hz, mechanical index: 1.1) can deliver agents into AC without damaging it. Using ultrasound, we delivered a drug surrogate down to a depth corresponding to 53% depth of the AC thickness without causing histologically detectable damage to the AC. This may be important because early osteoarthritis typically exhibits histopathologic changes in the superficial AC. In conclusion, we identify intense megahertz ultrasound as a technique that potentially enables localized non-destructive delivery of osteoarthritis drugs or drug carriers into articular cartilage. (E-mail: heikki.nieminen@helsinki.fi) © **2015 World Federation for Ultrasound in Medicine & Biology.**

Key Words: **Ultrasound, Drug delivery, Osteoarthritis, Cartilage repair.**

INTRODUCTION

About 10% of men and 18% of women over 60 y of age have osteoarthritis (OA) (Woolf and Pfleger 2003). It is painful for the patient, limits mobility and reduces quality of life. As there is no regenerative therapy for OA, the last treatment option is usually a total joint replacement.

Research on development of disease-modifying OA drugs has been active in recent decades (Pelletier and Martel-Pelletier 2007). Currently available drug therapies were developed under the limitation of poor localization, that is, systemic delivery or injections into the joint. However, OA lesions in articular cartilage (AC) can be very localized. Therefore, local administration of the drug could potentially enhance the therapeutic effect within the degenerated tissue while avoiding adverse effects elsewhere in the body (Wieland et al. 2005). For instance, although transforming growth factor TGF-β1 speeds up AC matrix regeneration by stimulating chondrocytes, it simultaneously inflames the synovial capsule and promotes osteophyte formation (Venkatesan et al. 2013). Non-destructive localized delivery of drugs into AC could, therefore, lead to new treatment strategies for OA therapy.

Small OA drug molecules such as glucosamine (∼179 Da) and diacerein (∼368 Da) can move relatively freely in and out of AC, resulting in short residence times. On the other hand, penetration of large molecules (≥45 kDa) into AC is limited (Maroudas 1976). A method to force either large molecules (*e.g.*, growth factors) or drug carriers containing small drug molecules into AC could contribute to localization and prolonged drug residence. This would potentially confine drug exposure and permit more personalized treatment than afforded by current drug techniques of delivery into AC. Clinical techniques to deliver drugs locally into AC are still to be developed, but a few studies have already attempted to force agents into AC by means of an electric field (Bajpayee et al. 2014), kilohertz ultrasound (Nieminen et al. 2012) and acoustic shock waves (Nieminen et al. 2013).

High-intensity ultrasound (HIU) can transport material through such phenomena as acoustic radiation force,

Address correspondence to: Heikki J. Nieminen, Department of Physics, University of Helsinki, POB 64, 00014 Helsinki, Finland. E-mail: heikki.nieminen@helsinki.fi

acoustic streaming and ultrasound–bubble interactions (Ahmed et al. 2009; Dayton et al. 2002). All these effects can potentially be harnessed to move agents locally inside porous materials such as AC. It is known that ultrasound can deliver agents into skin (Polat et al. 2011) and release encapsulated agents in tumor tissue (Grull and Langereis 2012). We have previously reported that low-frequency (20 kHz, 78 W/cm^2) ultrasound can deliver soot particles (in the nanometer to micrometer range), models for drug carriers, locally into AC (Nieminen et al. 2012). However, we observed microcratering of the AC surface possibly caused by inertial cavitation (Dalecki 2004). The risk of encountering this adverse phenomenon can be avoided by increasing the sonication frequency into the megahertz range. Therefore, the aim of this study was to illustrate that intense megahertz ultrasound enhances the penetration of a kDa-sized agent into AC without damaging the tissue.

METHODS

Samples

Bovine joints were obtained from a local meat refinery (Lihakonttori Oy, Helsinki, Finland). Cylindrical osteochondral plugs (samples 1–5, n = 5, diameter = 28 mm) were prepared from normal-looking femoral condyles, one sample per animal (Fig. 1). For damage assessment tests, we prepared paired osteochondral strips (samples 6–9[a, b], n = 8, width = 7 mm) from four joints with visually normal femoral condyles.

Ultrasound experiments and damage assessment

A custom-made 1.138-MHz focused ultrasound system (Fig. 2) (peak positive and peak negative pressure, along the acoustic axes, ±3 mm from the sample surface = 2.70 ± 0.06 and 1.18 ± 0.01 MPa, respectively; beam width = 5.7 mm at −6 dB of maximum peak pressure; I_{sptp} = 488 W/cm^2, I_{sppa} = 102 W/cm^2, I_{spta} = 5 W/cm^2; pulse repetition frequency = 285 Hz; cycles per pulse = 200; duty cycle = 5.0%; mechanical index [MI] = 1.1; immersion fluid/subchondral bone temperature <33°C) was used to deliver a drug surrogate (X-ray contrast agent: 1% w/v phosphotungstic acid [PTA], a negatively charged molecule, molecular weight = 2.88 kDa) into samples 1–5 as follows: First, the focus of the ultrasound beam was positioned at the AC surface; second, the sample was sonicated for 2.5 h. The contrast agent was dissolved in 70% ethanol for sample 1 because PTA in ethanol is used to label collagen in embryos (Metscher 2011). We chose phosphate-buffered saline (PBS) as base medium for samples 2–5 to provide a more physiologic-like environment.

For damage assessment (histopathologic assessment), one sample (a) each from sample pairs 6–9 was sonicated in PBS containing no PTA using the protocol described earlier (Fig. 1). The second sample (b) from sample pairs 6–9 was immersed, but not exposed to ultrasound and acted as a paired control. Samples were then subjected to histologic staining (Masson's trichrome and Safranin-O) to evaluate collagen and proteoglycan distributions, respectively. To evaluate potential ultrasound-induced damage to the AC, the excisions were optically imaged at 10× using a light microscope (Aristoplan, Ernst Leitz Wetzlar, Wetzlar, Germany) and camera (MicroPublisher 5.0 RTV, Qimaging, Surrey, BC, Canada), and at 1× using a microscope slide scanner (Pathscan Enabler IV, Meyer Instruments, Houston, TX, USA).

Ultrasound beam characteristics (peak positive/negative pressure amplitude, MI, beam width and intensity) were determined using a calibrated needle hydrophone (element diameter = 0.2 mm, tip diameter = 0.67 mm, Model HPM02/1, Precision Acoustics, Dorchester, UK). Intensity values (SPTP, SPPA, SPTA) were determined in ion-exchanged water at a distance from the transducer that corresponded to the position of the AC surface.

Detection of delivery

Samples 1–5 were imaged with X-ray microtomography (XMT) to determine PTA distribution within the tissue (Nanotom 180 NF, Phoenix X-ray Systems/GE, Fairfield, CT, USA; settings for sample 1: 75 kV, 190 μA, 1,080 projections, voxel side length = 38.0 μm; settings for samples 2–5: 75–80 kV, 75–110 μA, 1,200 projections, voxel side length = 16.3 to 16.7 μm). To avoid sample drying during XMT, the samples were kept in sealed containers containing cotton balls moistened with the base solution (70% ethanol for sample 1 or PBS for samples 2–5). The PTA distributions in AC were determined on the basis of X-ray attenuation in the XMT images. Raw data from samples presented in Nieminen et al. (2013) (samples 1 and 2) were reanalyzed and pooled into this study.

The penetration depth of PTA and thickness of AC were determined from reconstructed XMT image stacks (Fig. 3). AC without PTA (*i.e.*, volume 1) and AC with PTA (*i.e.*, volume 2) were segmented from the XMT image stack based on image contrast (Avizo Fire, Versions 7.1.1–8.0.1, FEI Visualization Sciences Group, Burlington, MA, USA). The local thickness of each volume was calculated with the LocalThickness plugin (Dougherty and Kunzelmann 2007) to the ImageJ software (Version 1.4.7, NIH, Bethesda, MD, USA), and projected onto a plane approximately tangential to the AC surface with the VGStudioMAX software (Version 1.3, Volume Graphics, Heidelberg, Germany). We named this the spatial maximum penetration map (SMPM).

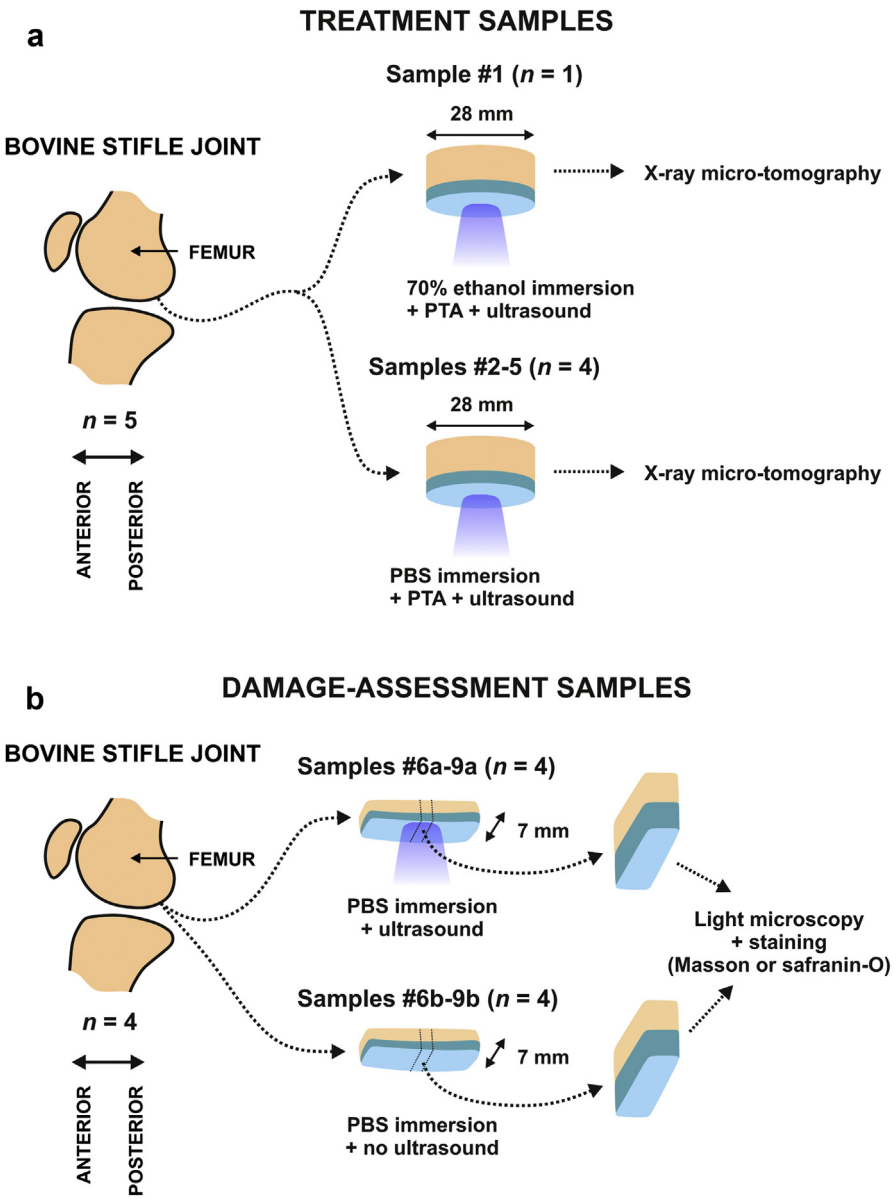

Fig. 1. Sample handling. Bovine articular cartilage samples were prepared for treatment (a) and for damage assessment (b). Five osteochondral cylinders were sonicated with MHz ultrasound while immersed in phosphotungstic acid (PTA) + 70% ethanol (sample 1) or PTA + phosphate-buffered saline (PBS) (samples 2–5) (a) (Fig. 2). For damage assessment, osteochondral tissue strips (width = 7 mm) were prepared from femoral condyle (b), one sample pair per joint. One sample from each joint was sonicated with megahertz ultrasound while immersed in PBS (samples 6a–9a) and the adjacent samples (samples 6b–9b) not sonicated acted as controls. Damage assessment samples were subjected to histology that is, Masson or Safranin-O staining and light microscopy.

Within the SMPM of samples 2–5, the delivery depth in the treatment area was defined as the mean ± standard deviation (SD) of the pixel values that were within 1-mm radius from the sample center. The delivery depth into adjacent tissue (control) was defined as the mean ± SD of pixel values that were inside a band 9.5–10.5 mm from the sample center. In addition, the global maximum of delivery depth within the SMPM was determined.

RESULTS

After sonication, we observed increased X-ray attenuation (*i.e.*, high PTA concentration) inside a circular penetration shape at the location of the ultrasound beam center in all samples (Fig. 4). For sample 1 (70% ethanol as base medium), the maximum delivery depth was 488 ± 15 μm (mean ± SD), with no delivery in adjacent

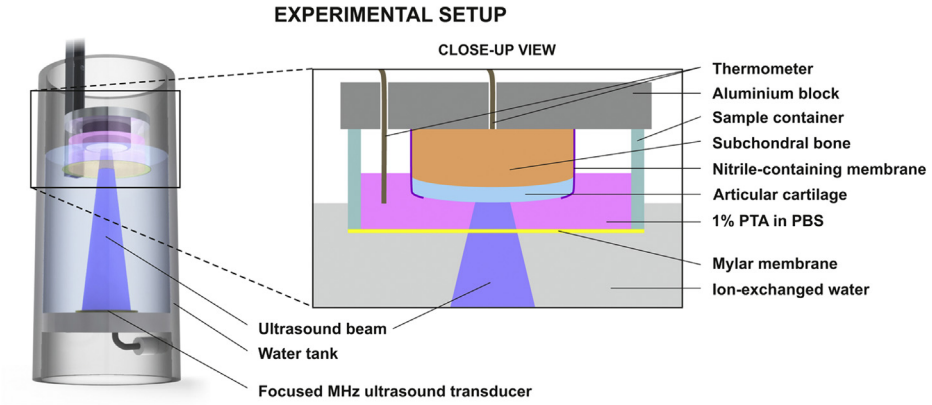

Fig. 2. Experimental setup. The sample was immersed in a contrast agent (phosphotungstic acid [PTA]), while sonicated with megahertz ultrasound. A thin nitrile-containing membrane prevented PTA penetration into the tissue from the side. PBS = phosphate-buffered saline.

tissue. This maximum delivery depth corresponded to 39% of the AC thickness and was achieved at an average penetration speed of 195 μm/h.

The delivery depths for samples 2–5 (immersed in PTA + PBS solution while sonicated) are summarized in Table 1 and Figures 4 and 5. For these samples, the average penetration depth of PTA at the treatment area was 2.6 times the penetration depth in the control tissue (Fig. 5). For samples with strong PTA penetration at the sample center, that is, samples 2, 3 and 5, the maximum penetration depths were 775, 883 and 754 μm, respectively (Fig. 4), corresponding to a relative penetration of 53 ± 4% and an average penetration speed of 322 μm/h. Sample 4 appeared to exhibit strong passive PTA diffusion outside the ultrasound beam; nevertheless, a circular PTA penetration pattern is seen at the location of the ultrasound beam, that is, sample center (Fig. 4f). Subchondral bone temperature remained below 33°C (n = 3).

Histologic evaluation of ultrasound-treated AC samples (6a–9a) and control samples (6b–9b) revealed no difference between the groups with respect to superficial tissue fibrillation or collagen (*blue contrast* in Masson's trichrome-stained sections) or proteoglycan (*red contrast* in Safranin-O-stained sections) distribution (Fig. 6).

DISCUSSION

The results suggest that intense megahertz ultrasound delivered the drug surrogate into AC. Because the applied ultrasound energy (1 MHz, 2.7/1.2 MPa peak positive/negative pressure amplitude at focus, I_{sptp} = 488 W/cm^2, I_{sppa} = 102 W/cm^2, I_{spta} = 5 W/cm^2) attenuates in soft tissue (Goss et al. 1979; Nieminen et al. 2009) and body fluids (Narayana et al. 1984), it may induce acoustic radiation forces in solids or at solid–fluid interfaces (Westervelt 1951) and fluid streaming (Nyborg 1953), potentially contributing to

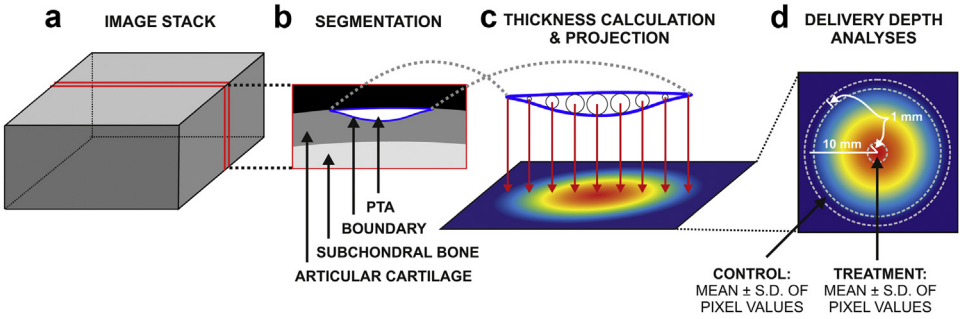

Fig. 3. Image analysis of the delivery depth. Osteochondral cylinders immersed in phosphotungstic acid (PTA) and sonicated with megahertz ultrasound were imaged using X-ray microtomography, producing a 3-D image stack (a). The delivered PTA was segmented out of articular cartilage based on image contrast (b) (*solid blue line* represents the boundary of the segmented volume). Spheres as large as possible in diameter were then placed inside the segmented volume (c). The maximum diameter values were projected on a plane parallel to the cartilage surface (c, d) representing the thickness of the segmented volume in this projection. Thickness values (mean ± standard deviation) at the sample center within 1-mm diameter represented the delivery depth within ultrasound beam (treatment) (d), whereas thickness values within a 1-mm band, from 9.5 to 10.5 mm relative to the sample center, represented delivery depth by passive diffusion (control).

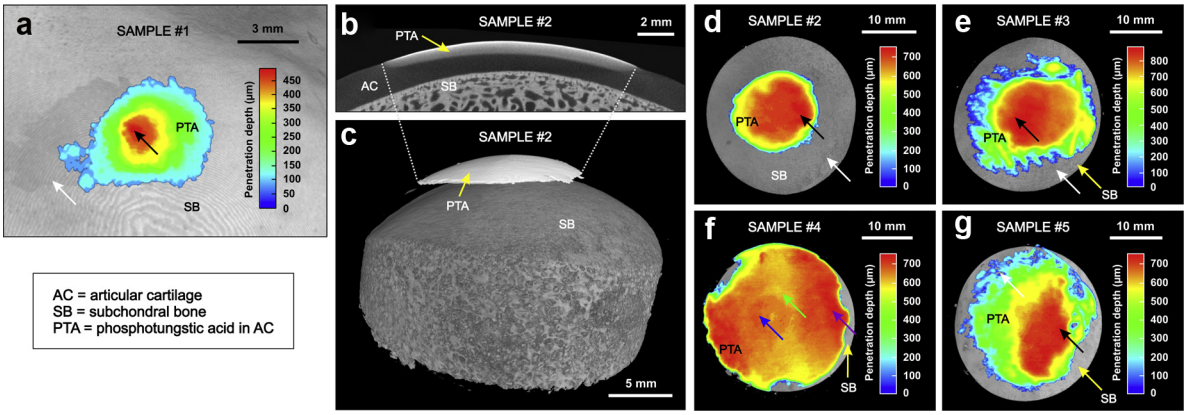

Fig. 4. Delivery outcome. Surrogate (phosphotungstic acid [PTA]) delivery was observed in X-ray microtomography (XMT) images of samples 1–3 and 5 (a–e, g) at the sample center (location of maximum delivery depth indicated with *black arrow*) compared with adjacent tissue (*white arrow*) after the sample was sonicated with intense megahertz ultrasound in surrogate immersion. In sample 4 (f), diffusion (potentially passive) is strong outside the ultrasound beam (*purple arrow*), but deeper delivery is seen at the sample center (*blue arrow*) compared with adjacent tissue (*green arrow*). The result suggests that ultrasound can deliver agents into articular cartilage and that the delivery is confined to the location of sonication.

mass transfer into and inside articular cartilage. The radiation pressure generated in water at the location of AC surface is on average ~680 Pa during one ultrasound burst. The resulting radiation force and PRF correspond to tapping the tissue 2.6 million times during the treatment. Specifically, stable cavitation (threshold for unstable inertial cavitation = 3.9 MPa peak negative pressure at 1 MHz [American Institute of Ultrasound in Medicine 2008]) is one possible explanation for the delivery; that is, ultrasound may excite micro- or nanobubbles to generate a streaming fluid around the bubbles (Ahmed et al. 2009). Such streaming could enhance the diffusion within the ultrasound beam. As we detected a temperature rise in the subchondral bone from room temperature to 33°C, it is possible that the temperature increase in AC enhances diffusion of delivered agents into and inside AC (Carsi et al. 2004).

The PTA delivery depth was relatively similar in all samples (excluding sample 4) and limited to a relatively confined round region (Fig. 4f). The difference in delivery can be due to biological variation, that is, permeability, which can vary with the biochemical composition of AC and from one joint to another. Permeability affects the speed of passive diffusion. The base solution was 70% ethanol for sample 1 and PBS for samples 2–5, which may impair the comparability of delivery in sample 1 to delivery in samples 2–5. PTA is a negatively charged molecule that is attracted by collagen. Therefore, we expected to see PTA penetration into the control tissue. Despite this, enhanced penetration at the sample center was evident compared with adjacent tissue.

Qualitatively, no histologic difference was observed in AC surface structure or in the content of collagen or proteoglycan between sonicated and non-sonicated samples (Fig. 6). Because of the low MI (1.1), we presumed that the exposure should be tolerable, as the MI does not exceed the U.S. Food and Drug Administration-defined maximum of 1.9 for clinical ultrasound imaging (Dalecki 2004). Previously we used 20-kHz HIU (Nieminen et al. 2012) to deliver particles into

Table 1. Penetration depth of PTA at the treatment location, the location of the global maximum and the control location for all samples immersed in PBS + PTA solution*

Sample	Treatment penetration depth (μm)	Control penetration depth (μm)	Penetration depth difference: Treatment − Control (μm)	Maximum penetration depth (μm)
2	742 ± 4	0 ± 0	742	775
3	869 ± 11	197 ± 211	672	883
4	654 ± 8	653 ± 65	1	734† (686)
5	684 ± 18	264 ± 186	420	754

PBS = phosphate-buffered saline; PTA = phosphotungstic acid.

* The treatment location values were calculated as the mean ± standard deviation of values within 1-mm radius from sample center. The control values were calculated as the mean ± standard deviation within a 1-mm band at a radial distance of 10 mm (from 9.5 to 10.5 mm) from the sample center. The numbers of pixels used to calculate delivery depth statistics were 11,213–11,873 and 183,662–202,668 for treatment and control, respectively.

† Maximum located outside the sample center. The maximum value at sample center is provided in parentheses.

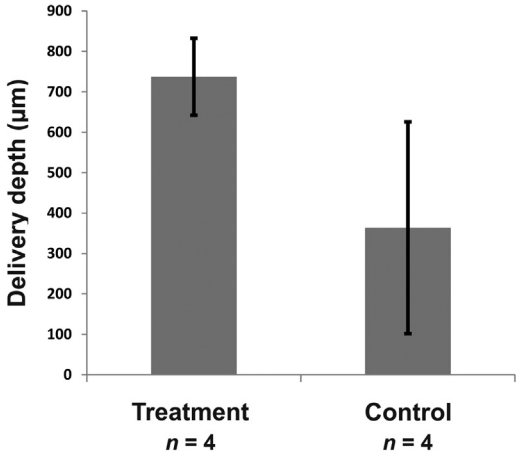

Fig. 5. Penetration depths. Penetration depths (mean ± standard deviation) at sample center (treatment) compared with adjacent tissue (control) (Fig. 3). The samples were immersed in phosphotungstic acid (PTA) + phosphate-buffered saline (PBS) solution, while sonicated with intense megahertz ultrasound.

osteochondral tissue; however, this induced superficial microcratering in the AC, because the pressure threshold for inertial cavitation is much lower at 20 kHz (*e.g.*, 68-kPa peak negative pressure [PNP] at 23 kHz [Birkin et al. 2005]) than at 1.138 MHz (3.9-MPa PNP at 1 MHz [American Institute of Ultrasound in Medicine 2008]). Absence of evident damage to the AC, therefore, suggests that megahertz ultrasound may be a preferable approach for drug delivery compared with kilohertz frequency ultrasound.

In humans, delivering PTA halfway through the cartilage thickness is potentially important, because early OA typically manifests as histopathologic changes (superficial fibrillation and clefts, loss in proteoglycans) in the superficial AC (Pritzker et al. 2006). The average delivery speed of the agent in this study, ~5 μm/min, suggests that agent delivery to the very superficial articular cartilage can be achieved with the proposed technique within a clinically acceptable time frame (on average

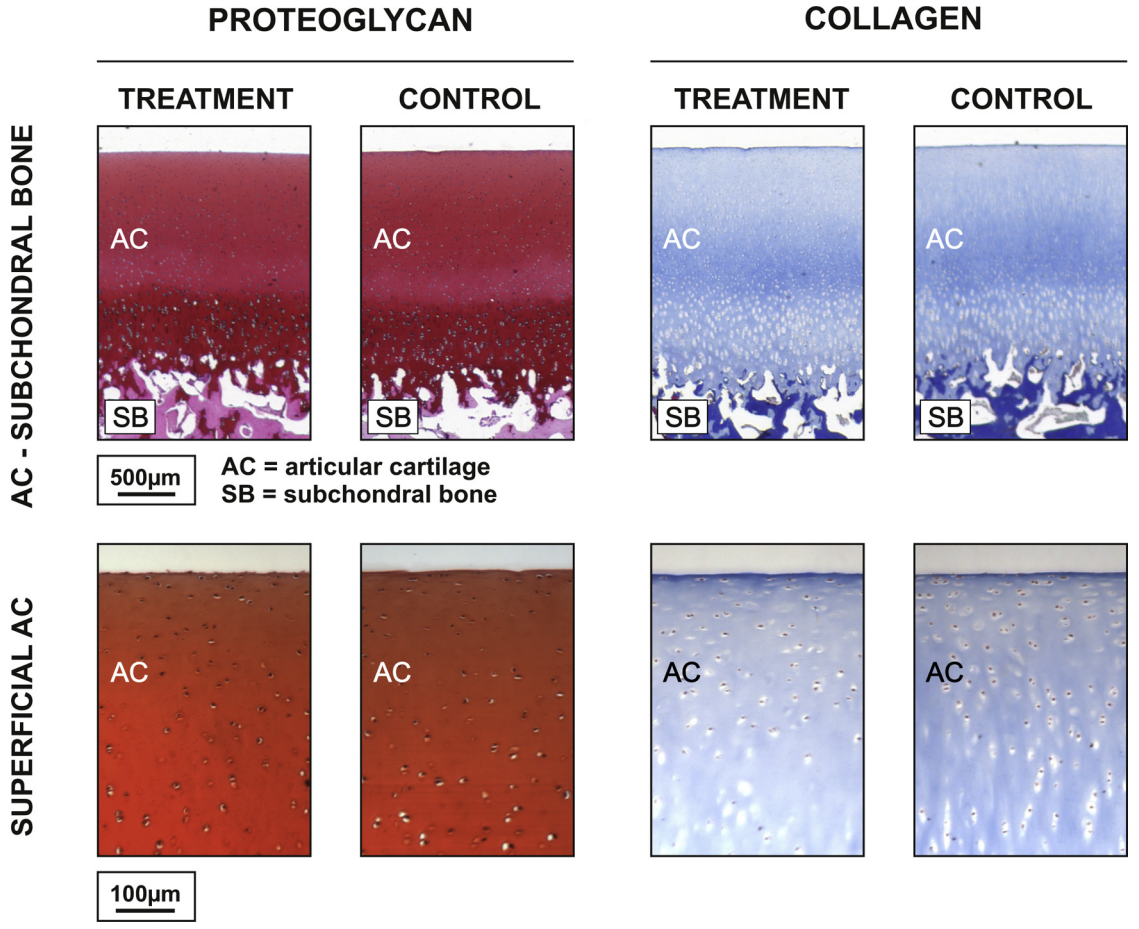

Fig. 6. Damage assessment. Typical histologic sections for damage assessment samples: ultrasound exposure (left) and no ultrasound exposure (right). We observed no difference in proteoglycan (Safranin-O staining) or collagen (Masson's trichrome staining) distribution or fibrillation in superficial articular cartilage between the different groups. This suggests that intense megahertz ultrasound did not induce evident damage to the articular cartilage.

an ~50 μm penetration depth in 10 min for a molecule or drug carrier equivalent to PTA). With respect to delivery of agent into deeper tissue, the delivery speed is currently too low for clinical relevance. In addition, bovine cartilage properties *in vitro* may differ significantly from human cartilage properties *in vivo*. Although the control tissue (sample edge) is less than one-third of the −6 dB beam width of the ultrasound, control tissue may have been subjected to ultrasound exposure and acoustic streaming affecting the control. Despite these limitations, the results are encouraging, with successful delivery without apparent damage. Further research is needed to identify the mechanisms of delivery, to enhance delivery speed, to confirm cell viability and to test the biological response of the proposed approach using OA drugs.

The proposed experimental setup was designed to study the capability of megahertz ultrasound to transport agents into articular cartilage. The technical realization of the potential clinical application could, however, differ significantly from that used in this study. Delivery with megahertz ultrasound could be applied not only extracorporeally, but also intra-articularly. An intra-articular approach would allow local administration of the drug or drug carrier enhanced by ultrasonic delivery. Examples of intra-articular approaches could be a catheter-based high-intensity focused transducer or a fiber optic photoacoustic ultrasound system, which because of their small size could fit into the joint cavity.

CONCLUSIONS

We have illustrated the ability of intense megahertz ultrasound to transport agents into articular cartilage without causing microscopically discernible histologic damage. Ultrasound, therefore, has the potential to deliver agents such as drugs and drug carriers into articular cartilage in a localized manner. At best, this approach could permit new treatment strategies for OA drug therapy and a paradigm shift in drug development of locally administered agents.

Acknowledgments—We thank the Academy of Finland (Projects 253579, 268378 and 273571) and the European Research Council under the European Union's Seventh Framework Programme (FP/2007-2013, ERC Grant Agreement 336267) for financial support. We are grateful to Lihakonttori Oy (Helsinki, Finland) for providing bovine knees. We warmly thank Dr. S. Adam Hacking, Ph.D. and Prof. Kenneth P. H. Pritzker, M.D., FRCPC for their constructive criticism. We are grateful to Mr. Alexander Meaney for assistance with the XMT imaging of sample 1. We thank Mr. Eetu Lampsijärvi, Mr. Jari Rinta-aho and Mr. Nestori Westerlund for assistance with experiments and Mr. Christoffer Fridlund for assistance in sample preparation. We are grateful to Ms. Ida Holopainen and Mr. Anton Nolvi, B.Sc. for their help in technical drawing.

REFERENCES

Ahmed D, Mao X, Shi J, Juluri BK, Huang TJ. A millisecond micromixer via single-bubble-based acoustic streaming. Lab Chip 2009; 9:2738–2741.

American Institute of Ultrasound in Medicine (AIUM). Statement regarding naturally occurring gas bodies. Accessed: 22 July 2014, statement approved: 8 November 2008. Available at: http://www.aium.org/officialStatements/6.

Bajpayee AG, Wong CR, Bawendi MG, Frank EH, Grodzinsky AJ. Avidin as a model for charge driven transport into cartilage and drug delivery for treating early stage post-traumatic osteoarthritis. Biomaterials 2014;35:538–549.

Birkin PR, Offin DG, Leighton TG. Experimental and theoretical characterisation of sonochemical cells: Part 2. Cell disruptors (ultrasonic horns) and cavity cluster collapse. Phys Chem Chem Phys 2005;7:530–537.

Carsi B, Lopez-Lacomba JL, Sanz J, Marco F, Lopez-Duran L. Cryoprotectant permeation through human articular cartilage. Osteoarthr Cartilage 2004;12:787–792.

Dalecki D. Mechanical bioeffects of ultrasound. Annu Rev Biomed Eng 2004;6:229–248.

Dayton PA, Allen JS, Ferrara KW. The magnitude of radiation force on ultrasound contrast agents. J Acoust Soc Am 2002;112:2183–2192.

Dougherty R, Kunzelmann KH. Computing local thickness of 3-D structures with ImageJ. Microsc Microanal 2007;13:1678–1679.

Goss S, Frizzell L, Dunn F. Ultrasonic absorption and attenuation in mammalian tissues. Ultrasound Med Biol 1979;5:181–186.

Grull H, Langereis S. Hyperthermia-triggered drug delivery from temperature-sensitive liposomes using MRI-guided high intensity focused ultrasound. J Control Release 2012;161:317–327.

Maroudas A. Transport of solutes through cartilage: Permeability to large molecules. J Anat 1976;122:335–347.

Metscher BD. X-ray microtomographic imaging of intact vertebrate embryos. Cold Spring Harbor Protoc 2011;2011:1462–1471.

Narayana P, Ophir J, Maklad N. The attenuation of ultrasound in biological fluids. J Acoust Soc Am 1984;76:1–4.

Nieminen HJ, Herranen T, Kananen V, Hacking SA, Salmi A, Karppinen P, Hæggström E. Ultrasonic transport of particles into articular cartilage and subchondral bone. Trans IEEE Int Ultrason Symp 2012;ID616:1869–1872.

Nieminen HJ, Salmi A, Rinta-aho J, Hubbel G, Wjuga K, Suuronen JP, Serimaa R, Hæggström E. MHz ultrasonic drive-in: Localized drug delivery for osteoarthritis therapy. Trans IEEE Int Ultrason Symp 2013;619–622.

Nieminen HJ, Zheng Y, Saarakkala S, Wang Q, Toyras J, Huang Y, Jurvelin J. Quantitative assessment of articular cartilage using high-frequency ultrasound: Research findings and diagnostic prospects. Crit Rev Biomed Eng 2009;37:461–494.

Nyborg WL. Acoustic streaming due to attenuated plane waves. J Acoust Soc Am 1953;25:68–75.

Pelletier JP, Martel-Pelletier J. DMOAD developments: Present and future. Bull NYU Hosp Jt Dis 2007;65:242–248.

Polat BE, Hart D, Langer R, Blankschtein D. Ultrasound-mediated transdermal drug delivery: Mechanisms, scope, and emerging trends. J Control Release 2011;152:330–348.

Pritzker KP, Gay S, Jimenez SA, Ostergaard K, Pelletier JP, Revell PA, Salter D, van den Berg WB. Osteoarthritis cartilage histopathology: Grading and staging. Osteoarthr Cartilage 2006;14:13–29.

Venkatesan JK, Rey-Rico A, Schmitt G, Wezel A, Madry H, Cucchiarini M. rAAV-mediated overexpression of TGF-beta stably restructures human osteoarthritic articular cartilage in situ. J Transl Med 2013;11:211.

Westervelt PJ. The theory of steady forces caused by sound waves. J Acoust Soc Am 1951;23:312–315.

Wieland HA, Michaelis M, Kirschbaum BJ, Rudolphi KA. Osteoarthritis: An untreatable disease? Nat Rev Drug Discov 2005;4:331–344.

Woolf AD, Pfleger B. Burden of major musculoskeletal conditions. Bull WHO 2003;81:646–656.